T2R2 東京科学大学 リサーチリポジトリ
Science Tokyo Research Repository

論文 / 著書情報
Article / Book Information

Title	An oxide-diluted magnetic semiconductor: Mn-doped ZnO
Authors	T. Fukumura,Z.-W. Zin,A. Ohtomo,H. Koinuma,M. Kawasaki
Citation	Applied Physics Letters, Vol. 75, No. 21,
Pub. date	1999, 11
URL	http://scitation.aip.org/content/aip/journal/apl
Copyright	Copyright (c) 1999 American Institute of Physics

Powered by T2R2 (Science Tokyo Research Repository)

An oxide-diluted magnetic semiconductor: Mn-doped ZnO

T. Fukumura,[a] Zhengwu Jin, A. Ohtomo, H. Koinuma,[b] and M. Kawasaki
Department of Innovative and Engineered Materials, Tokyo Institute of Technology, Yokohama 226-8502, Japan

(Received 19 July 1999; accepted for publication 24 September 1999)

Epitaxial thin films of an oxide-diluted magnetic semiconductor, Mn-doped ZnO, were fabricated by pulsed-laser deposition technique. Solubility of Mn into ZnO exceeds thermal equilibrium limit as a result of nonequilibrium film growth process. As Mn content is increased, the lattice constants of both *a* and *c* axes of wurtzite $Zn_{1-x}Mn_xO$ films ($x<0.35$) increase and the band gap expands although considerable in-gap absorption develops. Itinerant electrons over $10^{19}\,cm^{-3}$ can be doped into the $Zn_{1-x}Mn_xO$ films by Al doping, in contrast to low carrier density in the other II–VI diluted magnetic semiconductors. The temperature dependence of the resistivity is almost metallic and considerable magnetoresistance is observed at low temperatures. © *1999 American Institute of Physics.* [S0003-6951(99)03547-0]

Diluted magnetic semiconductor is expected to play an important role in interdisciplinary materials science and future electronics because charge and spin degrees of freedom accommodated into single matter resulting in interesting magnetic, magneto-optical, magnetoelectronic, and other properties. Among them, Mn-doped II–VI[1] and III–V[2] compound semiconductors have been extensively studied. The former has a variety of compounds consisting of various combinations of II-group cations and VI-group anions except for oxygen. Some of these materials have been applied to optical devices.[3]

Recently, one of the II–VI compound semiconductors, ZnO, has attracted revival attention since it was found that high quality epitaxial thin films display excitonic ultraviolet laser action at room temperature.[4] In addition, the energy gap of this compound can be extended up to ~4 eV by synthesizing alloy compounds of $Mg_xZn_{1-x}O$.[5] Heavy electron doping ($>10^{21}\,cm^{-3}$) was readily achieved in contrast to the other II–VI compound semiconductors.[6] Furthermore, the thermal equilibrium solubility of Mn is larger than 10 mol %[7] and the electron mass is as large as $\sim 0.3m_e$ where m_e is free electron mass. Therefore, the amount of injected spins and carriers into the film can be very large. When we take into account the Ruderman–Kittel–Kasuya–Yosida (RKKY) interaction, the above mentioned factors of $Zn_{1-x}Mn_xO$ favor strong correlation between spins and carriers. Here we report the fabrication of $Zn_{1-x}Mn_xO$ epitaxial films and their optical and magnetotransport properties.

$Zn_{1-x}Mn_xO$ films were deposited by pulsed-laser deposition. Prescribed amount of ZnO and Mn_3O_4 were mixed, calcined at 400 °C for 7 h, and sintered at 900 °C for 12 h in air for making ceramic targets. When we made conductive thin films, 1 mol % Al_2O_3 was also included in the target. The targets were ablated by KrF excimer laser pulses (248 nm, 10 Hz, 20 ns) with a fluence of 5 J/cm^2. The films with a thickness of several hundred nanometers were grown on polished sapphire (001) substrates at 600 °C in 5×10^{-5} Torr of oxygen pressure at a growth rate of ~0.01 nm/pulse. Conventional x-ray diffraction spectra of the films showed (002) and (004) peaks of wurtzite structure without any impurity peaks. The homogeneous distribution of Mn in the film was also confirmed by electron probe microanalysis (EPMA). The root mean square of the surface roughness was evaluated to be about 10 nm by an atomic force microscope. Inductively coupled plasma (ICP) spectroscopy and EPMA analyses confirmed that the Mn content in the films was approximately the same as that in the targets.

Figure 1 shows Mn content dependence of the lattice constants analyzed by a high-resolution four-circle x-ray diffractometer. Both the *a*- and *c*-axes lengths expand monotonously with the increase of Mn content up to $x=0.35$. The valence state of Mn ion was determined to be Mn^{2+} having spins of $S=5/2$ from electronic spin resonance measurements.[8] Therefore, the Mn ion is understood to have occupied the Zn site without changing the wurtzite structure far beyond the thermal equilibrium limit of $x\sim0.13$ at 600 °C.[7] The nonequilibrium nature of the growth process in pulsed-laser deposition enables us to obtain films with high Mn content exceeding the thermal equilibrium limit.

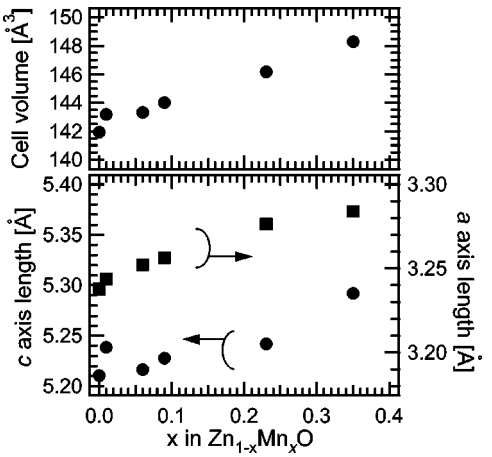


FIG. 1. Mn content dependence of cell volume (top) and *a*- and *c*-axes lattice constants (bottom) for $Zn_{1-x}Mn_xO$ films.

[a]Electronic mail: fukumura@oxide.rlem.titech.ac.jp
[b]Also at: Materials and Structures Laboratory of Tokyo, Institute of Technology and at CREST, Japan Science & Technology Corporation, Tokyo.

 © 1999 American Institute of Physics
Downloaded 27 Oct 2004 to 130.34.226.195. Redistribution subject to AIP license or copyright, see http://apl.aip.org/apl/copyright.jsp

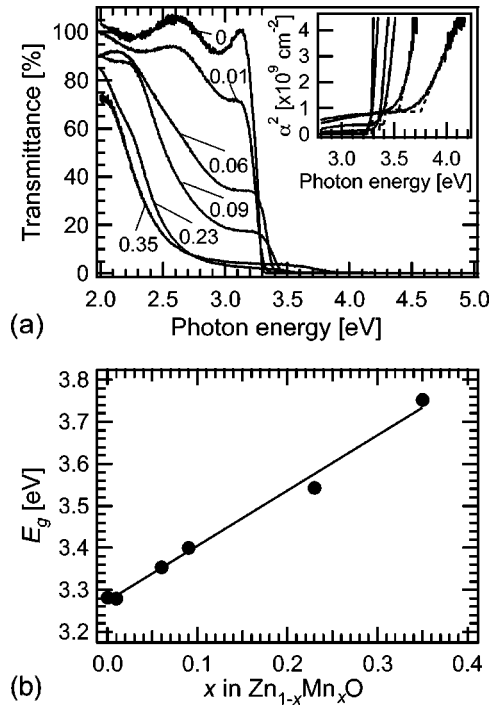


FIG. 2. (a) Transmittance spectra of $Zn_{1-x}Mn_xO$ films measured at room temperature for various x values. Numbers in the figure denote x. Inset: Photon energy dependence of α^2 for deducing band gap (E_g) from the intersection of the dotted lines. (b) Variation of E_g with Mn content. The solid line is a fitted line expressed as $E_g = 3.273 + 1.32x$ [eV].

Figure 2(a) shows optical transmittance spectra measured at room temperature. As Mn content is increased, the midgap absorption around 3 eV develops[7,9] and the absorption edge shifts toward higher energy side. For evaluating the band gap (E_g), the data are replotted in the inset by taking α^2 as vertical axis, where α is absorption coefficient. E_g in Fig. 2(b) defined from the intersection of the dotted extrapolated lines in the inset of Fig. 2(a) increases linearly with x. Such an expansion of E_g and development of midgap absorption by Mn were also observed in other ($A^{II}Mn)B^{VI}$ alloys. The dominant in-gap absorption was assigned as $^6A_1 \rightarrow {}^4T_2$ transition based on the reflectance spectra for ceramic specimens.[7] However, the absorption observed here is considerably large in spite of the spin forbidden $d-d$ transition, namely $^6A_1 \rightarrow {}^4T_2$ due to high spin d^5 electron configuration of Mn ion. The broken symmetry caused by large lattice distortion in wurtzite $Zn_{1-x}Mn_xO$ might contribute to the large oscillator strength of spin forbidden $d-d$ transition. However, the absorption takes place in wide energy range rather than a discrete peak. Therefore, it is more reasonable to assign this absorption to the charge–transfer transition between donor and/or acceptor ionization levels of Mn ions and the band continuum as indicated in calculated results of (ZnMn)S and (ZnMn)Se based on the Anderson impurity model.[10]

The $Zn_{1-x}Mn_xO$ films doped with Al were highly conductive and the type of the conducting carrier was confirmed to be n type by Hall measurements with Van der Paw configuration. Figure 3 shows temperature (T) dependence of resistivity (ρ) of an $x=0.19$ film ($n_c = 3.1\times10^{19}\,\mathrm{cm}^{-3}$) in various magnetic fields applied perpendicular to the film surface. As shown in the inset of Fig. 3, the carrier concentration and the mobility are almost constant as a function of T except for slight decrease in n_c below 50 K. Resistivity rapidly increases with decrease of T below 10 K in 0 T as the result of the reduction of n_c, and is substantially altered by applying magnetic field below ~50 K. Between 15 and 50 K, the resistivity monotonously increased as the magnetic field was increased. Below 15 K, the increase of resistivity was suppressed at high field, resulting in negative magnetoresistance at high field below 3 K.

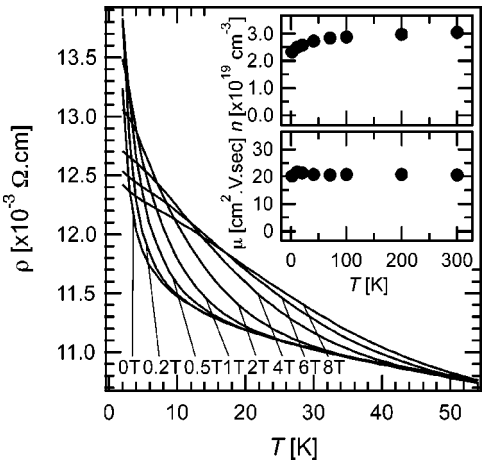


FIG. 3. Temperature dependence of resistivity in various magnetic fields for a $Zn_{0.81}Mn_{0.19}O$:Al film. Inset: Temperature dependence of carrier concentration (top) and mobility (μ) (bottom).

Isothermal magnetoresistance (MR) was measured both for $x=0$ film ($n_c = 9.6\times10^{18}\,\mathrm{cm}^{-3}$) and $x=0.19$ film at different temperatures. The results did not depend on the magnetic field direction with respect to the c axis of the film. The MR for $x=0$ film was weakly negative as shown in Fig. 4(a) similar to that observed in an accumulation layer in ZnO.[11] Figure 4(b) shows the MR curves for $x=0.19$ film. The MR behavior at 100–300 K was quantitatively similar to that of $x=0$ sample. The MR at 11–40 K is appreciably positive and keeps on increasing with decreasing T. At 2 K, the MR is positive in weak magnetic field less than ~1.5 T having a

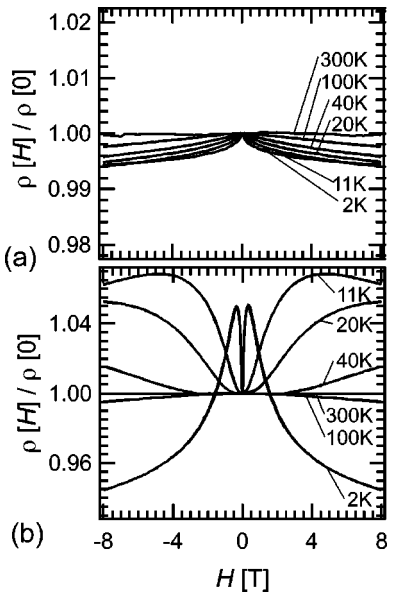


FIG. 4. Normalized magnetoresistance for (a) $x=0$ and (b) $x=0.19$ films as a function of magnetic field. The magnetic field was parallel to c axis.

Downloaded 27 Oct 2004 to 130.34.226.195. Redistribution subject to AIP license or copyright, see http://apl.aip.org/apl/copyright.jsp

sharp peak around ~0.3 T and turns into negative in a magnetic field more than ~1.5 T. The MR ratio $(\rho[H]-\rho[0])/\rho[0]$ is +5.0% at 0.3 T and −5.5% at 8 T at the lowest temperature measured at 2 K. The MR behavior observed at 2 K can be qualitatively explained as was reported earlier.[12,13] The positive MR at low field and the negative MR at high field were thought to come from the spin splitting enhanced by $s-d$ exchange interaction[12] and the rise of the Fermi level in the majority-spin subband due to the electron redistribution between the subbands,[13] respectively. The present measurements indicate that Mn doping provides localized spins interacting with conducting carriers in ZnO.

In conclusion, epitaxial films of oxide diluted magnetic semiconductor $Zn_{1-x}Mn_xO$ ($x<0.35$) were fabricated by pulsed-laser deposition resulting in homogeneous alloy films having localized Mn spin of $S=5/2$. The film having an electron carrier concentration as high as $10^{19}\,cm^{-3}$ showed both positively and negatively large MR which is absent in conducting ZnO films. The large in-gap absorption may open up an optically controlled magnetism in such a transparent oxide-diluted magnetic semiconductor.

The authors thank A. Fujimori, H. Hosono, H. Koshihara, H. Munekata, S. Oda, H. Ohno, and J. Yoshino for fruitful discussions and help for experiments. This work was conducted as JSPS research for the Future Program in the Area of Atomic-Scale Surface and Interface Dynamics (JSPS-RFTH-96P00205).

[1] J. K. Furdyna, J. Appl. Phys. **64**, R29 (1988).
[2] H. Ohno, Science **281**, 951 (1998).
[3] K. Onodera, T. Masumoto, and M. Kimura, Electron. Lett. **30**, 1954 (1994).
[4] Z. K. Tang, P. Yu, G. K. L. Wong, M. Kawasaki, A. Ohtomo, H. Koinuma, and Y. Segawa, Solid State Commun. **103**, 459 (1997).
[5] A. Ohtomo, M. Kawasaki, T. Koida, K. Masubuchi, H. Koinuma, Y. Sakurai, Y. Yoshida, T. Yasuda, and Y. Segawa, Appl. Phys. Lett. **72**, 2466 (1998).
[6] T. Minami, H. Sato, H. Nanto, and S. Takata, Jpn. J. Appl. Phys., Part 2 **24**, L781 (1985).
[7] C. H. Bates, W. B. White, and R. Roy, J. Inorg. Nucl. Chem. **28**, 397 (1966).
[8] T. Fukumura, M. Kawasaki, M. Mizuguchi, and H. Hosono, (unpublished); P. B. Dorain, Phys. Rev. **112**, 1058 (1958).
[9] W. B. White and K. E. McIlvried, Trans. Br. Ceram. Soc. **64**, 521 (1965).
[10] T. Mizokawa and A. Fujimori, Phys. Rev. B **48**, 14150 (1993).
[11] Y. Goldstein and Y. Grinshpan, Phys. Rev. Lett. **39**, 953 (1977).
[12] M. Sawicki, T. Dietl, J. Kossut, J. Igalson, T. Wojtowicz, and W. Plesiewicz, Phys. Rev. Lett. **56**, 508 (1986).
[13] T. Wojtowicz, T. Dietl, M. Sawicki, W. Plesiewicz, and J. Jaroszynski, Phys. Rev. Lett. **56**, 2419 (1986).

Downloaded 27 Oct 2004 to 130.34.226.195. Redistribution subject to AIP license or copyright, see http://apl.aip.org/apl/copyright.jsp